International Research Journal of Engineering and Technology (IRJET) e-ISSN: 2395-0056
Volume: 09 Issue: 11 | Nov 2022 www.irjet.net p-ISSN: 2395-0072

A New Voltage Balancing Converter for Neutral Point Clamped Multilevel Inverter with Fuzzy MPPT tracking for PV applications

Sulva Namratha, K. Naga Sujatha (Professor)

Dept. of Electrical and Electronics Engineering, JNTU College of Engineering, Hyderabad, India.

Abstract

In this paper, a grid connected photovoltaic system with Fuzzy MPPT tracking and a voltage balancing converter for NPC multilevel inverters is presented. By utilizing the appropriate switching states, all switched capacitors employed in this converter will be capable of effectively equalize the DC link capacitor's voltage. Without using the magnetic components, such balancing converter will be capable of raising the DC input voltage to the desired voltage level. This feature enables the converter to function while guaranteeing self-balancing while providing the ability to raise the input voltage to the appropriate output value.

The designed converter can be employed in a grid-connected solar photovoltaic system with a Neutral Point Clamped Multilevel inverter that is managed by a vector control method. To track the maximum power point of a Photovoltaic panel, fuzzy MPPT has been employed. Under fluctuating solar irradiances, an NPC MLI can extract the maximum power from a Photovoltaic panel and inject power to the grid with excellent dynamic and steady state performance. And the use of fuzzy MPPT makes the overall conversion very effective and produces least oscillations. MATLAB/ SimPowerSystem has been used to implement the developed grid-connected solar photovoltaic system with accompanying controllers and MPPT.

I. Introduction

Now-a-days the use renewable energy sources are increasing, there are different types of renewable energy sources are available. To integrate these different sources with the power grid, a stable method of interconnection is required. This interconnection is effectively obtained by using multilevel inverters, due to a number of benefits, including reduced harmonic distortions, lower standing voltage on transistors, better output signal quality, and tiny filter size.

There are principally three types of Multilevel inverters are available, they are Cascaded H-Bridge Neutral-Point-Clamped and Flying Capacitors. There are various issues with these MLIs, including: 1) CHB converters need numerous independent Dc voltage sources for their inputs [4], 2) FC MLIs struggle with balancing and having too many capacitors in higher levels of output voltage [5], and 3) Neutral point clamped MLIs also need multiple DC sources and struggle with balance issues because of their capacitor usage.

The issue of capacitor voltage equalization of NPC-MLIs has been solved using a number of ways, according to the available literature survey [14]. When redundant states are employed for voltage balancing and preserving output voltage within the desired range, the switching approach used in [15] to equalize the voltage of the capacitors. However, at higher voltages the inductor size is increased by the extra circuit necessary to equalize the capacitors' voltage, creating implementation difficulties. In parallel 3-phase and 1-phase NPC Multilevel inverters, voltage balancing method for DC link capacitors was provided in [16].

By connecting NPC Multilevel inverters in parallel, this technique allows for voltage balancing. The system in concern employs at least one converter that produces opposite voltage, which restricts the terminal voltage range and boosts the density of transistors at higher voltages. Zero sequence voltage injection is a suggested carrier based PWM technique in [17]. With this approach, capacitors' voltage may be balanced with the low frequency of switching and does not necessitate extra management. Though computationally challenging, this approach. [18] suggests a further approach to balancing the DC link voltage. This approach utilizes the RLC circuit, which necessitates the inclusion of magnetic components, making the device bigger. Several MPPT algorithms are proposed and some examples of these groups are as follows: There are many different types of approaches, including: 1) Perturbation and Observation method; 2) Incremental Conductance methods 3) Fuzzy logic and neural network-based methods.

The P & O method's primary flaw is that its operating point fluctuates around the Photovoltaic array's peak power point [30]. Additionally, the P & O approach nearly fails to identify the MPPT when the sun radiation changes quickly. The technique that relies on incremental conductance responds quickly in transient states but performs optimally in steady states with significant oscillations [31].

In this paper:

- NPC multilevel inverter topology solar photovoltaic system with fuzzy Maximum power point tracking being suggested, along with a step-up switching capacitor voltage balancing converter. By utilizing the appropriate switching states, this suggested converter is capable of successfully equalize the DC link capacitor's voltage.
- The implementation of Maximum power point tracking utilising a fuzzy logic controller aims to maximise the power from solar panels and minimise disturbances with in output signal.
- Without employing any magnetic components, the proposed design may increase its dc Input voltage to the necessary level of output voltage. This system uses lesser input voltage sources because it just needs one Dc supply or Photovoltaic array output to provide multi-level output.

II. System Architecture

The proposed grid-connected solar Photovoltaic System with a voltage balancing converter is shown in Fig. 1. It consists of a PV array, a proposed step up converter for stabilising the voltage of the capacitors, a 3-phase seven-level Neutral Point Clamped MLI with its controllers, an LC filter to reduce total harmonic distortion, a grid interface transformer and a power grid.

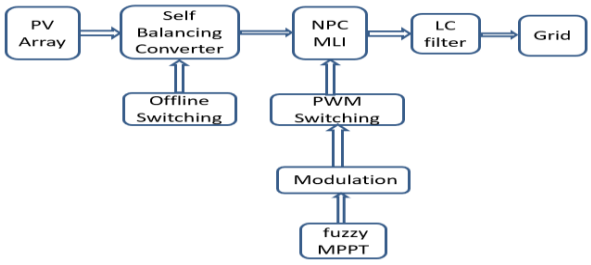

FIG 1. Block diagram of proposed system

The suggested step up balancing converter is supplied the output from the Photovoltaic system. When used as the intake to the seven level Neutral Point Clamped MLI, the balancing converter's output voltage is three times the PV voltage input. Through the use of a vector control system, the inverter is managed. The system tracks the maximum power point using fuzzy analysis. The reference DC link voltage comes from the MPPT controller's output. The d-axis current is supplied mostly by DC link voltage controller's output. Based on the necessary reactive power and d-axis grid voltage, the q-axis current is determined. Controlling the d-axis and q-axis currents, correspondingly, regulates the active/reactive power flowing into the grid.

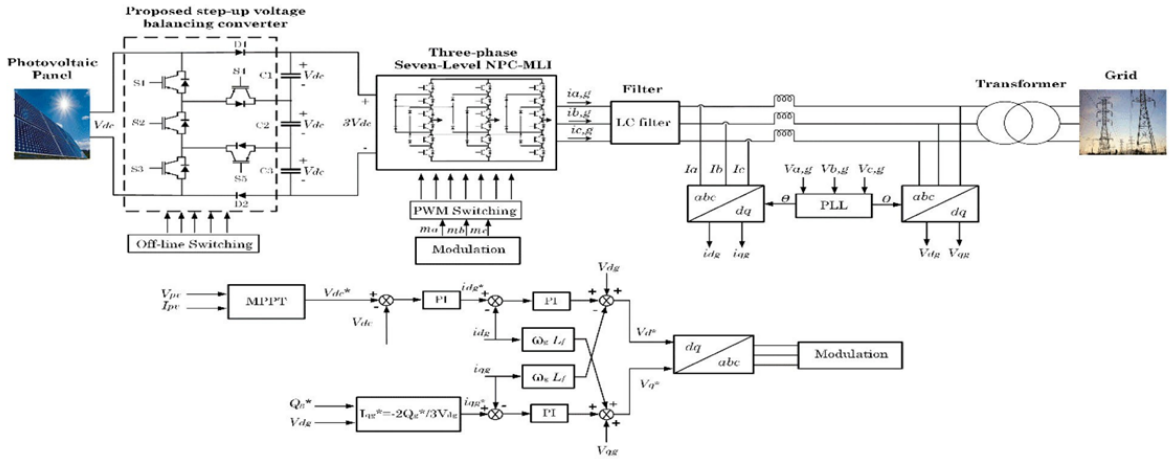

FIG 2. Block diagram of proposed system with control technique

III. Step-Up Balancing Converter

This converter is made up of two diodes, five semiconductor switches, and five capacitors. Each capacitor can be charged from a parallel connection to a DC source thanks to the way the converter is built. All capacitors must be charged to the same DC input voltage using the proper switching states, but all capacitors must be connected in series to produce the boosted output

voltage. All switching states for such hypothetical converter are displayed in Table 1.

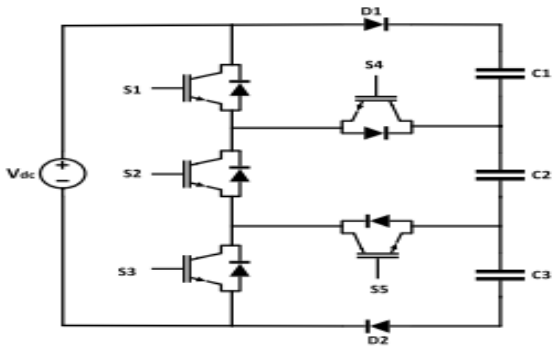

FIG 3. Balancing converter

TABLE 1. Switching states for balancing converter

Charging capacitor	On state switches	Conducting diodes
C_1	S_2, S_3, S_4	D_1
C_2	S_1, S_3	-
C_3	S_1, S_2	D_3

IV. Structure of a fuzzy logic system

Fuzzy logic control is known by its multi-rule-based resolution as well as multi-variable consideration for both linear and non-linear variations of parameters [31]. It has the ability to work with imprecise inputs as well. Fuzzy logic system consists of 4 units specifically; Fuzzification, Rule base, Inference engine and De-fuzzification [32].

In this work, we use the Mamdani approach [33] for which the principle is based on the selection of two input variables. In this framework, we propose the following two inputs:

The inputs of FLC are error (E(k)) and change in error (ΔE(k)), and FLC output is varying with duty cycle (ΔD(k)) which are defined by equations below. Mamdani based FIS is implemented in this paper.

$$E(k) = \frac{P(k)-P(k-1)}{V(k)-V(k-1)} \quad (1)$$

$$\Delta E(k) = E(k) - E(k-1) \quad (2)$$

$$\Delta D(k) = D(k) - D(k-1) \quad (3)$$

Fuzzification

Crisp values will become fuzzy quantities through fuzzification [34]. Fuzzy subsets are used to assign membership function values to the linguistic variable. Membership function plots of the two inputs and the output are shown individually in figure 3. The two inputs are fused into the Mamdani model to get required change in duty cycle.

Inference

By establishing membership rules throughout this step, logical connections between the inputs and outputs are made [34]. Generally, inference engine contains fuzzy rule base and fuzzy implication sub-blocks. Rule base contains set of rules assigned to carry out different output depending on the inputs provided (Table2).

De-fuzzification

In contrast to fuzzification, the process of defuzzification involves turning fuzzy subassemblies into numerical quantities. Centre of gravity defuzzification is the technique used to assess the outcome of the suggested FLC (COG).

The Seven linguistic variables used here are: Negative Big (NB), Negative Medium (NM), Negative Small (NS), Zero Equal (ZE), positive Small (PS), Positive Medium (PM) and Positive Big (PB).

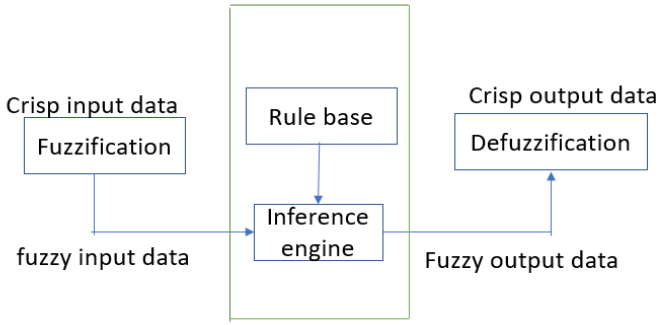

FIG 4. Block diagram of fuzzy controller

TABLE 2. Rule base of Proposed FLC

e	*o*						
	NB	**NM**	**NS**	**ZE**	**PS**	**PM**	**PB**
NB	ZE	ZE	ZE	PB	PM	PM	PB
NM	NS	ZE	ZE	PB	PM	PM	PM
NS	ZE	PS	ZE	NS	PS	PM	PM
ZE	PS	PS	ZE	ZE	ZE	NS	NS
PS	NM	NM	NS	NS	ZE	ZE	ZE
PM	NM	NM	NM	NM	ZE	ZE	ZE
PB	NB	NB	NB	NB	ZE	ZE	ZE

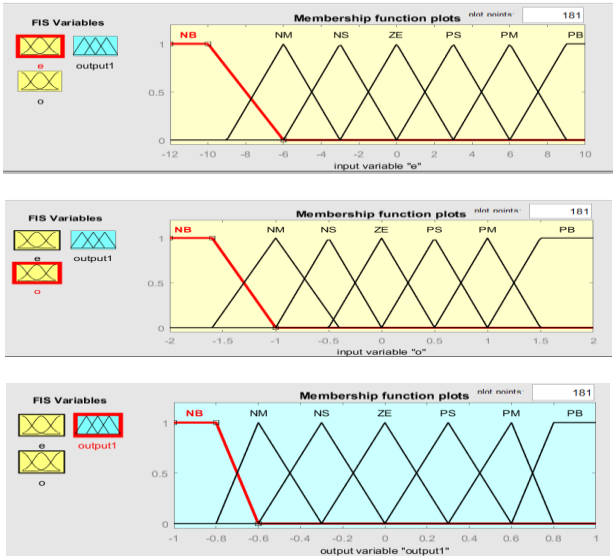

FIG 5. Membership functions for the fuzzy logic controller's inputs and outputs

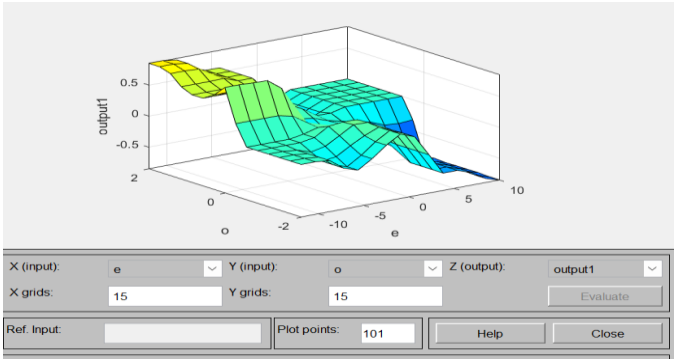

FIG 6. Graphical representation of fuzzy rules

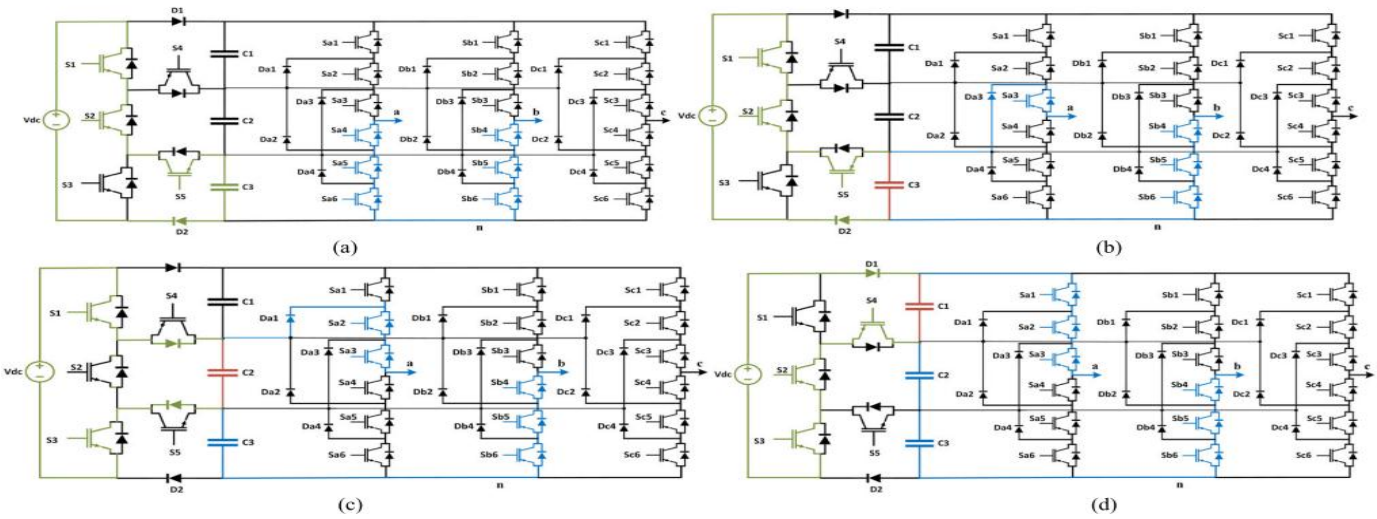

FIG 7. (a) Charging State of C_3 when $V_{ab} = 0$ (b) Charging State of C_3 when $V_{ab} = 1V_{dc}$ (c) Charging State of C_2 when $V_{ab} = 2V_{dc}$ (d) Charging State of C_1 when $V_{ab} = +3V_{dc}$

As can be seen, capacitors must be charged to their full potential, which is equivalent to an input DC voltage ($1V_{dc}$). By coupling the balancing network and the Neutral Point Clamped converter, it is possible to enhance and balance the voltage.

It is obvious that the green colour represents the charging path, the blue colour the discharging path, and the red colour the capacitors that are simultaneously charging and discharging. Additionally, Fig. 7 (a) shows the V_{ab} = 0 state. It is important to note that each capacitor can be charged one additional time compared to other capacitors. The state of the capacitors' balancing determines which capacitor must be charged once more.

In Fig. 7(b), capacitor C_3 is simultaneously charging and the voltage level between terminals "a" and "b" is $+1V_{dc}$. The capacitor C_2 is going to charge as indicated by the voltage level across points ab equalling $V_{ab} = +2V_{dc}$ (Fig. 7(c)). Fig. 7 also displays the capacitor C_1's charging status and the terminal voltage value of $+3V_{dc}$ (d).

V. Control Strategy

Fig. 1 depicts the grid side multilevel inverter's control structure. The grid linked converter employs the vector control technique. The following methods can be used to obtain the reactive and active power provided to the grid:

$$P_g = 3.V_g\ I_g \cos \emptyset \quad (4)$$

$$Q_g = 3.V_g\ I_g \sin \emptyset$$

where V_g, I_g, and $\emptyset$ stand for the grid's average phase voltage, average current, and average power factor angle, respectively. The carrier-based PWM technique is applied to the inverter with in grid connected Photovoltaic, as explained in the next section. The following are the d- and q-axis voltages:

$$V_{dg} = V_{d1} - R_f i_{dg} - L_f \frac{di_{dg}}{dx} + \omega L_f i_{qg} \quad (5)$$

$$V_{qg} = V_{q1} - R_f i_{dg} - L_f \frac{di_{qg}}{dx} + \omega L_f i_{dg} \quad (6)$$

The reactive and active power could be stated as follows if such voltage vector is parallel to the d-axis, V_{qg}= 0, and V_{dg}= V_g.

$$P_g = \frac{3}{2}\left(V_{dg}\, i_{dg}\right) = \frac{3}{2}\left|V_g\right| i_{dg} \quad (7)$$

$$Q_g = \frac{3}{2}\left(V_{dg}\, i_{qg}\right) = \frac{3}{2}\left|V_g\right| i_{qg} \quad (8)$$

The aforementioned equations demonstrate that we may easily regulate the reactive and active power by adjusting the q-axis and d-axis currents.

VI. Modulation Technique

To achieve the voltage output with seven levels utilising the right switching frequency, a carrier based PWM scheme is selected. In order to generate switching pulses and a seven-level output voltage, six triangular carrier waveforms are used, together with a reference voltage.

$$E = \frac{m-1}{2} V_{dc} \quad (9)$$

at m_a = 1, the RMS fundamental line to line voltage is:

$$V_{(AB,LL)} = 0.612(m-1)E \quad (10)$$

VIII. Comparison

A. Comparative analysis with traditional DC-DC converters

Parameter	Traditional DC-DC	7-Level DC-DC	Proposed converter
Number of levels	1	4	4
Number of PV sources	1	3	1
Number of DC-link Capacitors	1	3	3
Balancing capability	NO	NO	YES
Number of switches	1	3	5
Number of diodes	1	3	2
Number of inductors	1	3	NA

B. Comparison with existing models

- The incremental conductance-based algorithm provides a quick reaction in transient conditions but performs optimally with significant oscillations in constant conditions.
- The P&O technique of MPPT has the disadvantage that, in steady state, the voltage level oscillates about the MPP, leading to the loss of some available energy.
- • FLC has the benefit of being reliable and very simple to construct, and it does not necessitate perfect understanding of the regulator. There is no oscillation in this algorithm; it operates at the best point. It is also distinguished by good conduct while in a fleeting state.
- The Fuzzy control algorithm converges quickly and without oscillation
- The output power as well as voltage derived from the fuzzy logic based MPPT system are greater than those acquired from a traditional solar module.
- The greatest application of fuzzy logic has been its ability to function with imprecise inputs with no need for an accurate mathematical model and able to deal with nonlinearity.

IX. Simulation Results

Through a rigorous simulation analysis using MATLAB/SimPowerSystem, the proposed approach of integrating solar PV systems with the grid is thoroughly validated in this part. In this simulation, the suggested converter topology is used to study a 1.14 kw grid-connected solar PV system.

Parameter values

- PV Module: BIPV054-T86
- 28.8V Voltage at MPP (V_{MPP}),6.6A MPP Current (I_{MPP})

- The entire PV array consists of 1 string with a Total Power of 1.14kW @ 172.8 V and a string made up of 6 modules.
- Switching Frequency: 5 KHz.
- The Sampling time: 50µs.
- Output Frequency: 50 Hz.
- Capacitor Value: 4700 µf.
- Output filter: L= 12 mH and C = 2.5 µf.
- The irradiations are varied as follows - 200 W/m2 (0<t<1.2s), 400 W/m2 (1.2s<t<2.4s) ,600 W/m2 (2.4s<t<3.6s) ,800 W/m2 (3.6s< t<4.8), 1000 W/m2 (4.8s<t<6s), 800 W/m2 (6s<t<7.2s) ,600 W/m2 (7.2s<t< 8.4s) ,400 W/m2 (8.4s<t<9.6s), 200 W/m2 (9.6s<t<10s)

Fig. 8-19 displays the simulation study's results in terms of responses. The balanced output of the three phase NPC-MLI in Figure 8 serves as a demonstration of the developed converter's ability to balance voltage. The diagram shows where each phase voltage has three levels in each of the positive and negative half-cycles, plus one zero level, for a total of seven levels. The phase currents of a, b and c Phases of the MLI has been shown in Fig. 9.

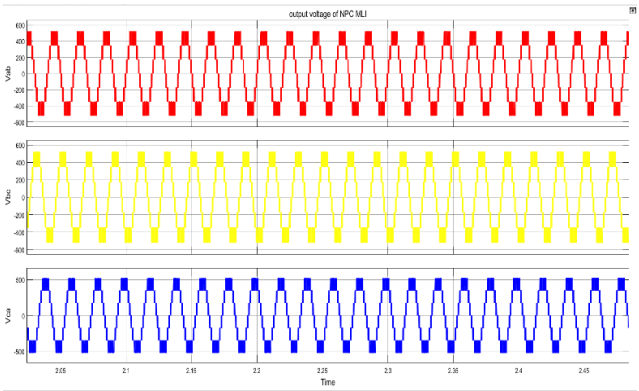

FIG 8. Simulation results for Output Voltage of NPC-MLI

Figs. 10, 11, and 12 show, respectively, the voltage and current of the PV array as well as the voltages across the DC link capacitor. Fig. 10 shows that the reference and actual PV voltages change as well as the Photovoltaic voltage for MPPT at various irradiances.

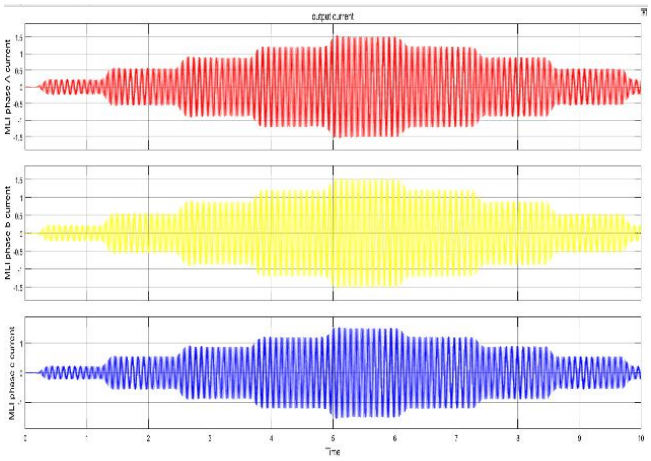

FIG 9. Output Current of NPC MLI

In the other words, the Photovoltaic array voltage monitors the needed MPPT voltages with the changing irradiance to ensure that the highest possible amount of solar power is extracted, comprehensively validating the system.

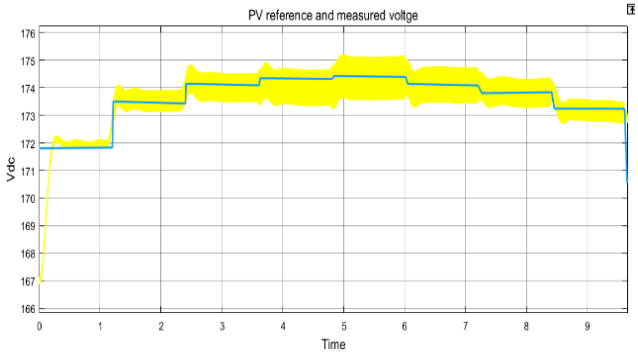

FIG 10. Simulation Results for PV Reference and Measured voltage

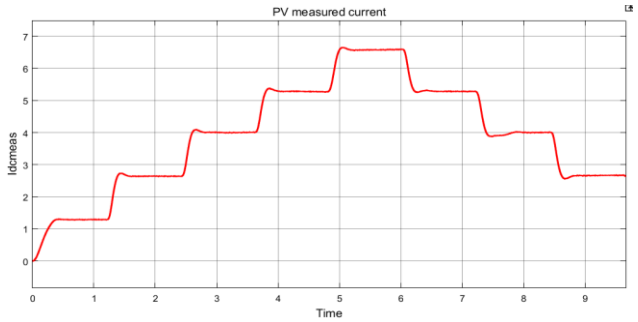

FIG 11. Simulation Results for PV's Measured Current

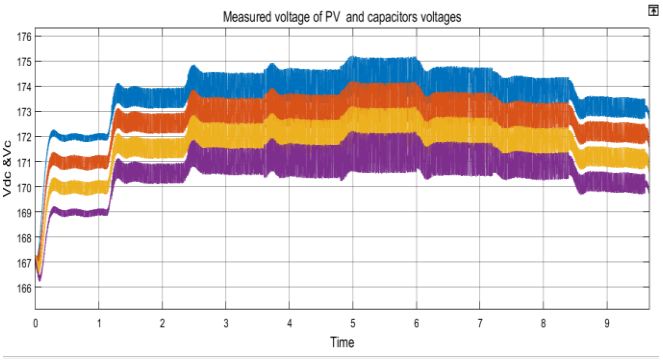

Fig 12. Measured Voltage of PV and Capacitors Voltages

Figure 13 displays the currents and voltages of switches S_1, S_2, and S_3 with in voltage balancing converter.

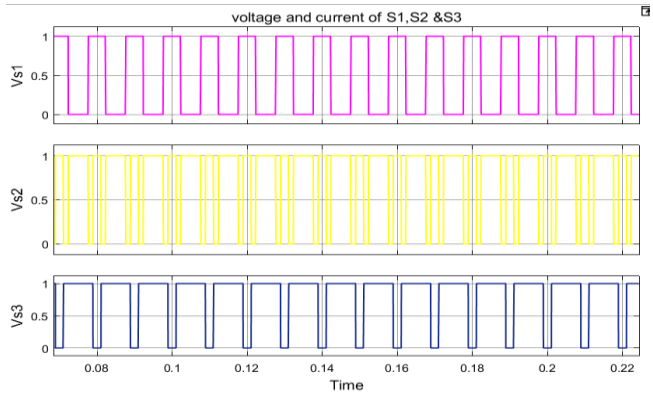

FIG 13. Voltage and current of S_1, S_2 and S_3

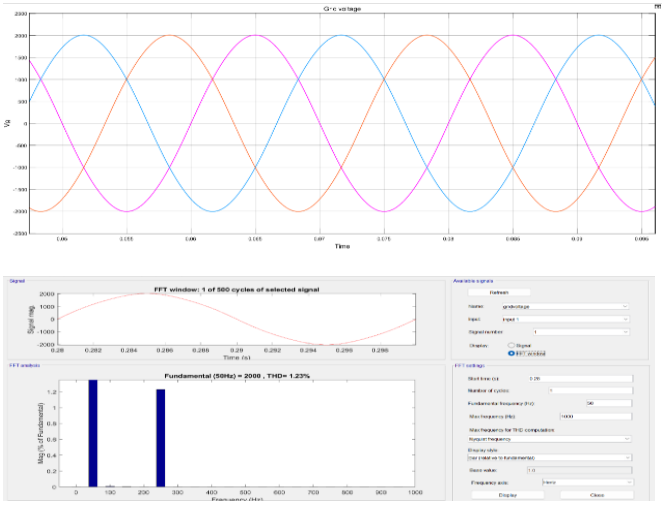

FIG 14. Simulation results for Grid voltage in 1000 w/m2 irradiances and its FFT analysis.

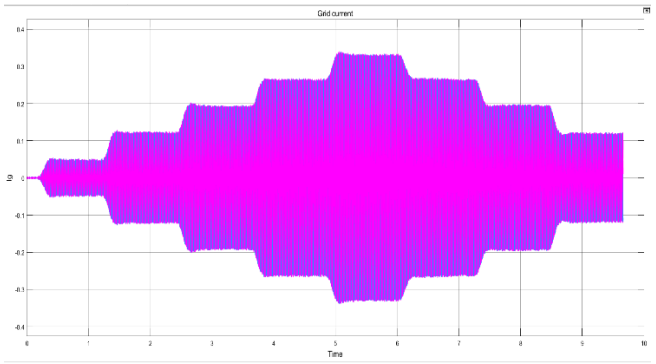

FIG 15. Simulation Results Grid Current under different irradiances

Figures 14 and 15, which show the 3-phase grid current and voltage, respectively, validate the voltage balancing & boosting with the better power quality in grid linked operation. The current response indicates that the ac current going to the grid varies in response to changing irradiation levels and ensures export of the maximum amount of solar power under varying weather conditions (Fig. 18).

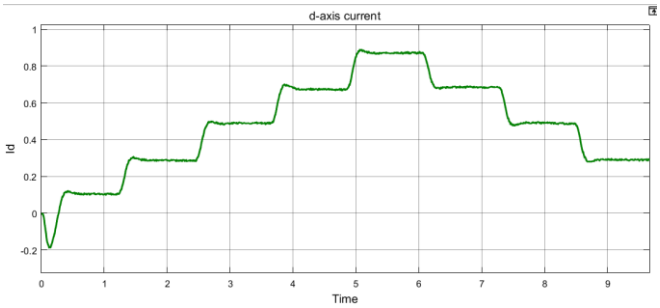

FIG 16. Simulation Results for d-axis Current under different irradiations.

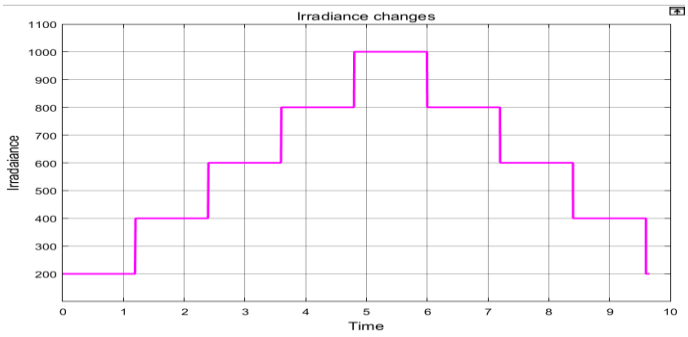

FIG 17. Irradiance changes

The tracking of the d-axis current is depicted in Fig. 16 and indicates that current is closely tracking the necessary reference value to guarantee the transfer of the greatest amount of solar energy to the grid. Additionally, Figs. 18 and 19 depict the power

transmission to a grid (Figure. 18 at 25°; Fig. 19 at 45°) in response to changes in temperature and irradiance (Fig. 16).

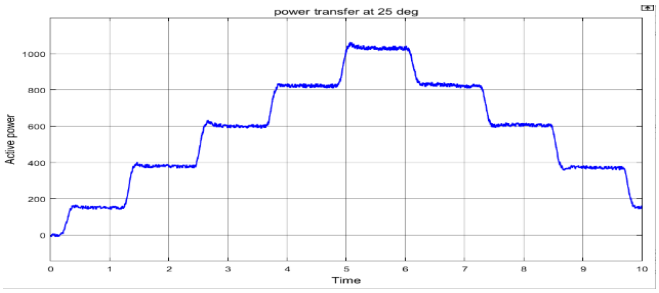

FIG 18. Power transfer to the grid at temperature 25˚c under different irradiations

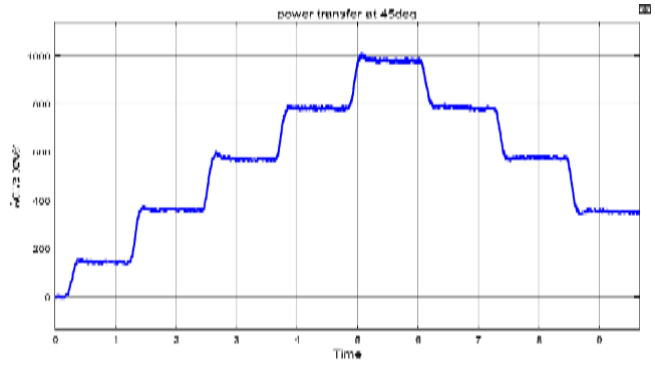

FIG 19. Power transfer to the grid at temperature 45˚c under different irradiations

X. Conclusion

This research has created a brand-new step-up voltage balancing converter in photovoltaic solar systems that is appropriate for NPC-MLI. The created converter not only increases the input PV voltage to the appropriate output level, but it also eliminates the magnetic components, lowering the system's weight and cost. Additionally, producing multi-level output only needs one Dc supply or PV array output, which lowers the quantity of input voltages needed in such systems.

According to the simulation results, the designed topology using fuzzy MPPT can efficiently equalize the DC-link voltage, collect the most power possible from PV modules, and inject electricity into the grid under a range of solar irradiances with excellent steady-state and dynamic performances. As a result, it's been demonstrated that controllers of this type also manage stable functioning.

References

1) P. R. Bana, K. Panda, R. T. Naayagi, Siano, G. Panda, ‘‘Recently developed reduced switch multilevel inverter for renewable energy integration and drives application: Topologies, comprehensive analysis and comparative evaluation,’’ IEEE Access, vol. 7, pp. 54888–54909, 2019.

2) S. Shuvo, E. Hossain, T. Islam, A. Aqib, S. Padmanabhan, and M. Z. R. Khan, ‘‘Design and hardware implementation considerations of modified multilevel cascaded H-Bridge inverter for photovoltaic system,’’ IEEE Access, vol. 7, pp. 16504–16524, 2019.

3) F. Z. Peng, ‘‘A generalized multilevel inverter topology with self-voltage balancing,’’ IEEE Trans. Ind. Appl., vol. 37, no. 2, pp. 611–618, Mar./Apr. 2001.

4) A. Taghvaie, J. Adabi, and M. Rezanejad, ‘‘A self-balanced step-up multilevel inverter based on switched-capacitor structure,’’ IEEE Trans. Power Electron., vol. 33, no. 1, pp. 199–209, Jan. 2018.

5) V. Dargahi, A. K. Sadigh, M. Abarzadeh, S. Eskandari, and K. A. Corzine, ‘‘A new family of modular multilevel converter based on modified flying-capacitor multicell converters,’’ IEEE Trans. Power Electron., vol. 30, no. 1, pp. 138–147, Jan. 2015.

6) J. Shen, S. Schroder, R. Rosner, and S. El-Barbari, ‘‘A comprehensive study of neutral-point self-balancing effect in neutral-point-clamped three-level inverters,’’ IEEE Trans. Power Electron., vol. 26, no. 11, pp. 3084–3095, Nov. 2011.

7) A. Nabae, I. Takahashi, and H. Akagi, ‘‘A new neutral-point-clamped PWM inverter,’’ IEEE Trans. Ind. Appl., vol. IA-17, no. 5, pp. 518–523, Sep. 1981.

8) A. Tripathi and G. Narayanan, ‘‘Torque ripple minimization in neutral point-clamped three-level inverter fed induction motor drives operated at low-switching-frequency,’’ IEEE Trans. Ind. Appl., vol. 54, no. 3, pp. 2370–2380, May 2018.

9) W. Zeng, R. Li, and X. Cai, ‘‘A new hybrid modular multilevel converter with integrated energy storage,’’ IEEE Access, vol. 7, pp. 172981–172993, 2019.

10) M. H. Ahmed, M. Wang, M. A. S. Hassan, and I. Ullah, ‘‘Power loss model and efficiency analysis of three-phase inverter based on SiC MOSFETs

for PV applications,'' IEEE Access, vol. 7, pp. 75768–75781, 2019.

11) B. R. Lin and T. C. Wei, ''A novel NPC inverter for harmonics elimination and reactive power compensation,'' IEEE Trans. Power Del., vol. 19, no. 3, pp. 1449–1456, Jul. 2004.

12) H. Akagi, H. Fujita, S. Yonetani, and Y. Kondo, ''A 6.6-kV transformer less STATCOM based on a five-level diode-clamped PWM converter: System design and experimentation of a 200-V 10-kVA laboratory model,'' IEEE Trans. Ind. Appl., vol. 44, no. 2, pp. 672–680, Mar. 2008.

13) H. Xiao and S. Xie, ''Transformer less split-inductor neutral point clamped three-level PV grid-connected inverter,'' IEEE Trans. Power Electron., vol. 27, no. 4, pp. 1799–1808, Apr. 2012. VOLUME 8, 2020 83951 A. Taghvaie et al.: New Step-Up Switched-Capacitor Voltage Balancing Converter

14) N. Celanovic & D. Boryevich, ''A comprehensive study of neutral point voltage balancing problem in 3-level neutral-point-clamped voltage source PWM inverters,'' IEEE Trans. Power Electron., vol.fifteen no. 2, pp. 242–249, Mar. 2000.

15) A. Nami, F. Zare, A. Ghosh, & F. Blaabjerg, ''A hybrid cascade converter topology with series-connected symmetrical & asymmetrical diode-clamped H-Bridge cells,'' IEEE Trans. Power Electron., vol. 26, no. 1, pp. 51–65, Jan. 2011.

16) R. Stala, ''A natural DC-link voltage balancing of diode-clamped inverters in parallel systems,'' IEEE Trans. Ind. Electron., vol. 60, no. 11, pp. 5008–5018, Nov. 2013.

17) J. Pou, J. Zaragoza, S. Ceballos, M. Saeedifard, and D. Boroyevich, ''A carrier-based PWM strategy with zero-sequence voltage injection for a three-level neutral-point-clamped converter,'' IEEE Trans. Power Electron., vol. 27, no. 2, pp. 642–651, Feb. 2012.

18) R. Stala, ''Application of balancing circuit for DC-link voltages balance in a single-phase diode-clamped inverter with two three-level legs,'' IEEE Trans. Ind. Electron., vol. 58, no. 9, pp. 4185–4195, Sep. 2011.

19) A. Nami, F. Zare, A. Ghosh, and F. Blaabjerg, ''Multi-output DC–DC converters based on diode-clamped converters configuration: Topology and control strategy,'' IET Power Electron., vol. 3, no. 2, pp. 197–208, 2010.

20) V. Yaramasu, B. Wu, M. Rivera, and J. Rodriguez, ''A new power conversion system for megawatt PMSG wind turbines using four-level converters and a simple control scheme based on two-step model predictive strategy— Part I: Modeling and theoretical analysis,'' IEEE J. Emerg. Sel. Topics Power Electron., vol. 2, no. 1, pp. 3–13, Mar. 2014.

21) V. Yaramasu, B. Wu, M. Rivera, and J. Rodriguez, ''A new power conversion system for megawatt PMSG wind turbines using four-level converters and a simple control scheme based on two-step model predictive strategy— Part II: Simulation and experimental analysis,'' IEEE J. Emerg. Sel. Topics Power Electron., vol. 2, no. 1, pp. 14–25, Mar. 2014

22) Y. Chen and K. Smedley, ''Three-phase boost-type grid-connected inverter,'' IEEE Trans. Power Electron., vol. 23, no. 5, pp. 2301–2309, Sep. 2008.

23) P. Kolahian, H. Tarzamni, A. Nikafrooz, and M. Hamzeh, ''Multi-port DC–DC converter for bipolar medium voltage DC micro-grid applications,'' IET Power Electron., vol. 12, no. 7, pp. 1841–1849, Jun. 2019.

24) A. Taghvaie, M. E. Haque, S. Saha, and M. A. Mahmud, ''A new step-up voltage balancing circuit for neutral-point-clamped multilevel inverter,'' in Proc. IEEE Int. Conf. Power Electron., Drives Energy Syst. (PEDES), Dec. 2018, pp. 1–6.

25) S. Saha, M. E. Haque, C. P. Tan, and M. A. Mahmud, ''Sensor fault resilient operation of permanent magnet synchronous generator-based wind energy conversion system,'' IEEE Trans. Ind. Appl., vol. 55, no. 4, pp. 4298–4308, Jul. 2019.

26) J. I. Leon, S. Vazquez, and L. G. Franquelo, ''Multilevel converters: Control and modulation techniques for their operation and industrial applications,'' Proc. IEEE, vol. 105, no. 11, pp. 2066–2081, Nov. 2017.

27) B. Wu, ''Cascaded HBridge multilevel inverters,'' in High-Power Converters and AC Drives. Hoboken, NJ, USA: Wiley, 2006, pp. 119–142.

28) Y. C. Fong, S. R. Raman, Y. Ye, and K. W. E. Cheng, ‘‘Generalized topology of a hybrid switched-capacitor multilevel inverter for high-frequency AC power distribution,’’ IEEE J. Emerg. Sel. Topics Power Electron., early access, Mar. 15, 2019, doi: 10.1109/JESTPE.2019.2905421.

29) P. Barbosa, P. Steimer, J. Steinke, M. Winkelnkemper, and N. Celanovic, ‘‘Active-neutral-point-clamped (ANPC) multilevel converter technology,’’ in Proc. Eur. Conf. Power Electron. Appl., Sep. 2005, p. 10.

30) H. Rezk, M. Aly, M. Al-Dhaifallah and M. Shoyama, "Design and Hardware Implementation of New Adaptive Fuzzy Logic-Based MPPT Control Method for Photovoltaic Applications", *IEEE Access*, vol. 7, pp. 106427-106438, 2019.

31) S. Z. Mirbagheri, S. Mekhilef, and S. M. Mirhassani, “MPPT with Inc. Cond method using conventional interleaved boost converter,” Energy Procedia, vol. 42, pp. 24–32, 2013.

32) R. Sankar, S. Velladurai, R. Rajaraman and J. A. Thulasi, "II. PV system description: Maximum power extraction in PV system using fuzzy logic and dual MPPT control", *International Conference on Energy Communication Data Analytics and Soft Computing (ICECDS),* pp. 3764-3769, 2017.

33) H. Rezk, M. Aly, M. Al-Dhaifallah and M. Shoyama, "Design and Hardware Implementation of New Adaptive Fuzzy Logic-Based MPPT Control Method for Photovoltaic Applications", *IEEE Access*, vol. 7, pp. 106427-106438, 2019

34) Priyabrata Shaw et al., "Modelling and control of a battery connected standalone photovoltaic *system",* 2016 IEEE 1st International Conference on Power Electronics Intelligent Control and Energy Systems (ICPEICES), *2016.*